crystalline $Al_{85}Y_8Ni_5Co_2$ alloys.

Experimental

Ribbons of $Al_{85}Y_8Ni_5Co_2$ (nominal composition) were produced by meltspinning. The thickness of the ribbons was about 30μm and the width about 2mm. Only ribbons that passed the ductility test - bending 180° without fracture - were used for further investigations.

Differential Scanning Calorimetry was performed on a SEIKO DSC 220C instrument at a heating rate of 10 °C/min. The ribbons were cut in pieces for X-ray diffraction and transmission electron microscopy investigations and heat treated using the DSC. Eight different temperatures were chosen from the continous DSC scan curve (240, 250, 260, 280, 300, 310, 340, 400 °C). The specimens were heated to the actual temperature at a rate of 10°C/min followed by isothermally annealing for 15 min and then rapidly cooled to room temperature.

The specimens were examined by X-ray diffraction with Cu K_α radiation. TEM-specimens were prepared by electropolishing in 1/3 HNO_3 and 2/3 methanol. The thin foils were examined in a Philips CM30 microscope at an operating voltage of 300kV. The instrument is equipped with an EDAX system for energy dispersive X-ray analysis (EDS) and a Gatan PEELS system for electron energy loss spectroscopy.

Results and Discussion

Figure 1 shows the DSC curve from scanning the amorphous AlYNiCo-ribbons from room temperature to 450°C. One endothermal reaction (glass transition) and three exothermal reactions are observed. The actual annealing temperatures are marked.

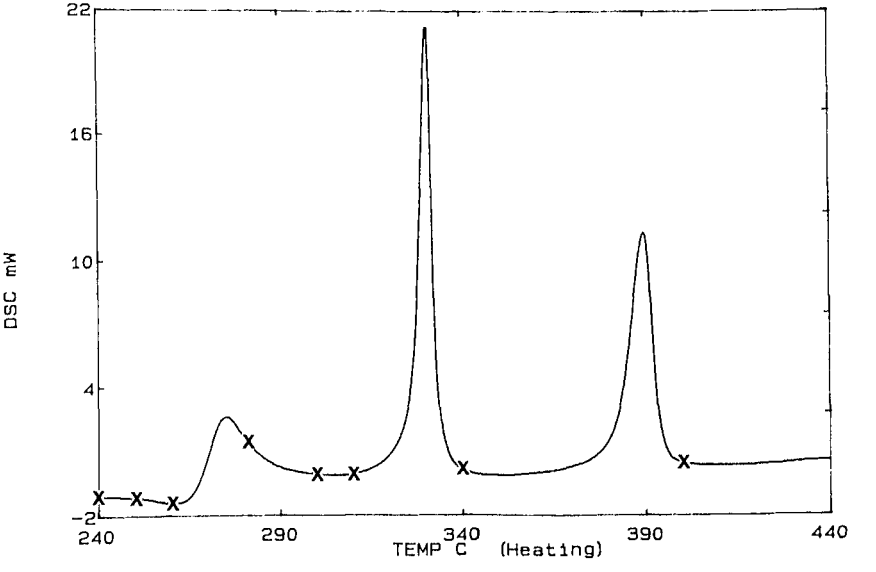

Figure 1. DSC curve from $Al_{85}Y_8Ni_5Co_2$.

The DSC curves from the heat treated materials show that the samples have gone through the following reactions:

240°C:	No reaction
250°C:	Endothermal reaction
260°C:	Endothermal reaction
280°C:	Endothermal and 1st exothermal reaction
300°C:	Endothermal and 1st exothermal reaction
310°C:	Endothermal, 1st and 2nd exothermal reaction
340°C:	Endothermal, 1st and 2nd exothermal reaction
400°C:	Endothermal, 1st, 2nd and 3rd exothermal reaction

TEM investigations of the as solidified ribbons show that they are fully amorphous with a small amount of thick oxide particles (size ~μm). The composition of the melt spun ribbons has been measured by both optical spectroscopy and micro probe analysis. The results confirm the nominal composition within the uncertainty. Table 1 shows the composition of the as solidified amorphous matrix as analysed by EDS.

Table I. Composition [at%] measured by EDS in the as solidified thin film.

t [nm]	Al	Y	Ni	Co
130	81.2	8.4	7.9	2.5
190	82.6	8.3	6.7	2.4
300	83.3	8.2	6.2	2.3

The composition differs significantly from that measured by optical spectroscopy and microprobe analysis. We observe that the composition gets closer to the correct one for larger thicknesses. We ascribe this to a surface layer of alloying elements caused by electropolishing. There is also a possible error from the theoretical k-factors used. But in this work we are only concerned about the relative differences in composition of the formed phases so we have not investigated this problem further.

After annealing at 240°C for 15 min the material is still fully amorphous. This can be seen both from X-ray- and electron-diffraction and microscopy. The EDS results are the same as for the as solidified ribbons.

Both XRD and TEM of the ribbons heat treated at 250°C show that the phases present are an amorphous and a face centered cubic phase. The size of the precipitates are 20-30nm and the morphology is dendrite like. The crystals are too small for reliable EDS analyses. The lattice parameter is (4.060 ± 0.005)Å determined by XRD. This is close to the lattice parameter of pure Al. The lattice parameter does not change significantly with the different annealing temperatures - it stays larger than the lattice parameter of pure Al. The phase is considered to be a supersaturated Al-phase with the alloying elements substituting Al, [1]. The Y-atom is larger than Al and the Ni- and Co-atoms are smaller resulting in a unit cell very close to that of pure Al.

Figure 2a shows a bright field micrograph of material annealed at 260°C showing the precipitates in the amorphous matrix. The electron diffraction pattern in Figure 2b shows that the phases

present are the amorphous phase and a polycrystalline fcc phase. The precipitate density is higher than in the former and the size of the precipitates is larger - 30-60nm. The dendritic morphology indicates a diffusion controlled growth.

EDS analyses were obtained from the precipitates and the amorphous matrix between the precipitates and the results are given in Table II. There are significantly lower concentrations of alloying elements in the fcc Al-particles than in the amorphous matrix. The numbers given are the mean value and standard deviation from several precipitates and the surrounding matrix. The EDS analyses are from the thinnest part of the TEM-specimen to asure that the precipitates extend through the entire thickness of the sample. Especially the Ni and also the Co contents are too high. This could be a result of the surface layer from the preparation of the thin foils.

Table II. Composition [at%] of the Al-rich fcc precipitates and the amorphous matrix measured by EDS.

	Al	Y	Ni	Co
fcc precipitate	83.1 ± 1	7.6 ± 0.5	7.0 ± 0.6	2.3 ± 0.6
amorphous matrix	78.5 ± 2	8.6 ± 0.4	10.0 ± 2	2.9 ± 0.3

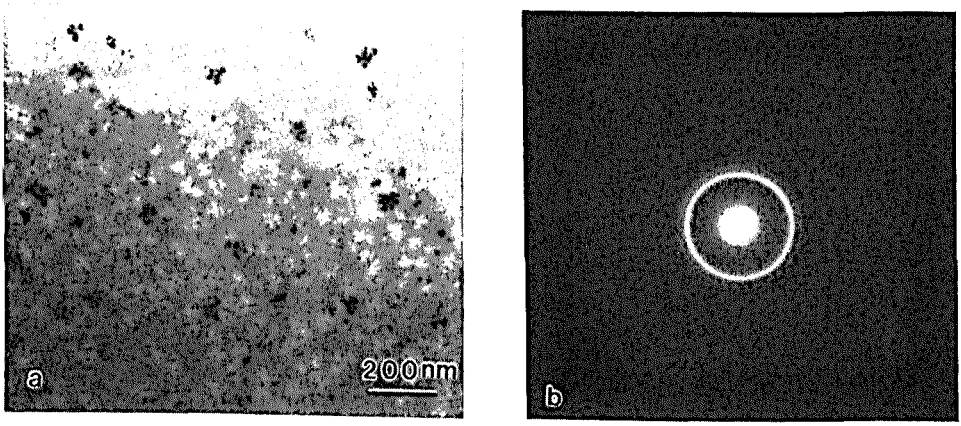

Figure 2. a) BF micrograph showing fcc Al-rich precipitates in amorphous matrix after 260°C annealing. b) Electron diffraction pattern.

After 280°C annealing the microstructure consist of the fcc Al-phase and still an amount of amorphous phase. The size of the precipitates is about the same as in the 260°C annealed ribbons but the density is higher.

Figure 3b shows the electron diffraction pattern from the material heat treated at 300°C showing the rings from the fcc Al-phase and some reflections from intermetallic phases. The dark field micrograph in Figure 3a is taken with the objective aperture around (111) and (200) from the Al-phase including some reflections from the intermetallic phases. The small bright spots in Figure 3a are intermetallic precipitates in the amorphous matrix and the larger ones are the fcc Al-

phase.

The ribbons heat treated at 300°C consist of fcc Al-precipitates, a small amount of amorphous phase and a few intermetallic particles. The morphology of the Al-precipitates is still the same but the size now reaching up to 80nm.

After scanning to 310°C the DSC curve shows that the second exothermal reaction has started in the material. No amorphous phase can be detected from the TEM investigations. It is no longer possible to distinguish the different Al-precipitates. They have grown into each other and formed a comlex structure. There is a significant amount of unidentified intermetallic particles.
The material annealed at 340°C has completed the second exothermal reaction. The microstructure and the diffraction pattern of this material are shown in Figure 4. The phases present are the fcc Al-phase, no amorphous phase and some intermetallic phases. The morphology of the Al-precipitates is a complex dendrite like structure. The intermetallic phases have a smoother surface and more regular morphology.

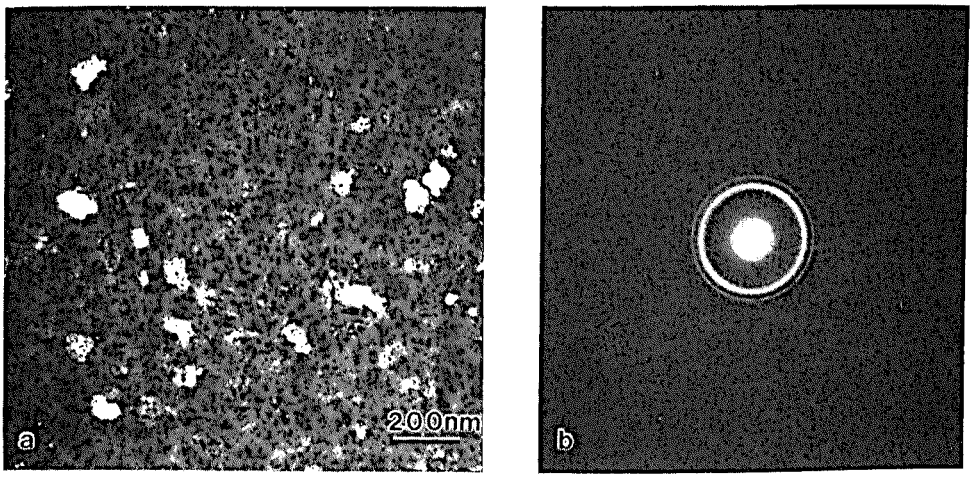

Figure 3. a) Dark field micrograph of (111) and (200) rings of fcc Al-phase including some reflections from the intermetallic phases from the material annealed at 300°C. b) Electron diffraction pattern.

The material heat treated at 400°C has gone through the third exothermal reaction. Figure 5 shows an electron diffraction pattern and a bright field micrograph from these ribbons. Several intermetallic phases have formed. Among these phases are Al_3Ni, Al_9Co_2 and some metastable phases with large unit cells. There is still a considerable volume fraction of Al-phase -the morphology now more regular and less supersaturated (91.6at%Al, 0.8at%Co, 2.9at%Ni, 4.7at%Y). The lattice parameter of the Al-particles is not significantly changed.

In situ heat treatment in TEM of the as solidified ribbons has also been performed. The heating rate was 10°C/min. Holding the specimen at 280°C for 15 min results in precipitation of fcc Al-phase with the dendritic morphology. This happens only in rather thick parts of the specimen (t>300nm). The thinner parts remain amorphous. When the specimen is heated to 340°C and

held for 15 min, more Al-rich precipitates are formed also in the thinner parts of the specimen. The morphology is the same as in the ribbons heat treated in the DSC at 340°C. Along the edge of the hole in the TEM-specimen there is an amorphous band about 1μm wide and t<50nm. Heating the specimen to 400°C and holding for 15 min results in precipitation and growth of intermetallic phases - the same phases as in the ribbons annealed in the DSC at 400°C.

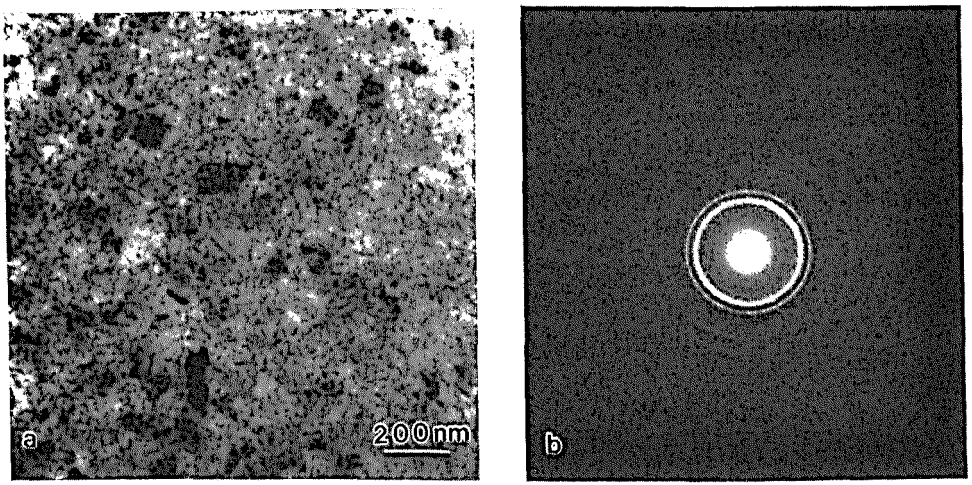

Figure 4. a) BF micrograph from the material annealed at 340°C showing intermetallic particles with regular morphology in addition to the dendritic-like α-Al phase. b) Electron diffraction pattern.

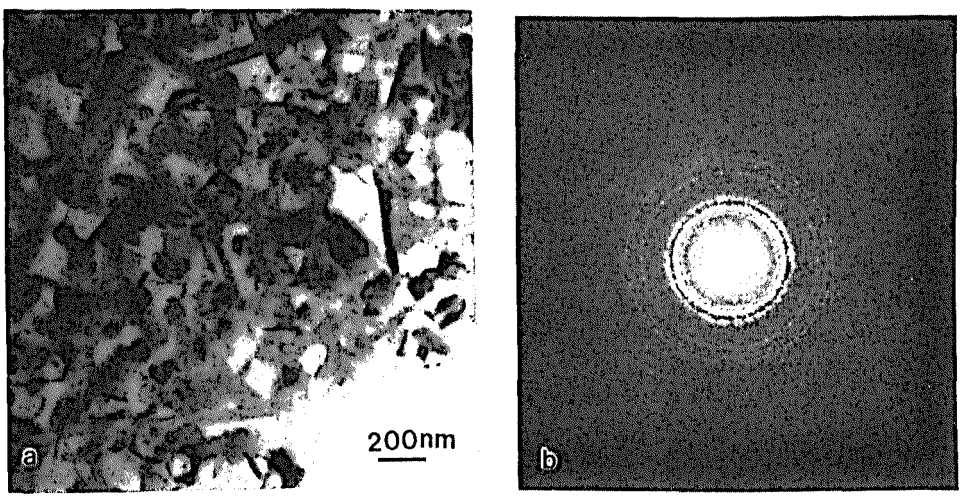

Figure 5. a) BF micrograph showing the microstructure after 400°C annealing. Several intermetallic phases have grown from the fcc-Al-phase. b) Electron diffraction pattern.

Conclusions

The endothermal reaction with an onset temperature of about 240°C is a transformation of the amorphous material to a supercooled liquid. In this supercooled liquid the nucleation of a supersaturated fcc Al-phase takes place.

The first exothermal reaction with an onset temperature of 260°C is precipitation and diffusion controlled growth of fcc Al in the amorphous matrix. The dendrite like precipitates contain less alloying elements than the surrounding matrix. The growth of the particles is probably stopped by solute accumulation at the interface.

310°C is the onset temperature of the second exothermal reaction. During this reaction intermetallic phases precipitate and grow. Because of the precipitation of the intermetallic phases the fcc Al-phase proceed to grow. The result is a fully crystalline material containing fcc Al-phase and a small volume fraction of unidentified intermetallic phases.

After the third exothermal reaction with an onset temperature of 360°C the material contains intermetallic phases and a less supersaturated Al-phase. Some of the intermetallic phases from the second exothermal reaction transform into other intermetallic phases.

References

1. A. Inoue, K. Othera, A.P. Tsai and T. Masumoto, Japanese Journal of Applied Physics, Vol. 27, No. 4, (1988), 479.

2. A. Inoue, N. Matsumoto and T. Masumoto, Materials Transactions, JIM, Vol. 31, No. 6, (1990), 493.

3. L. Arnberg, M. Sivertsen and M. Johnsson, Melt spinning and Strip Casting: Research and Implementation, (1992), 19.